77

ELSEVIER

Experimental assessment of bridge deck panels strengthened with carbon fiber sheets

Hongseob Oh[a,*], Jongsung Sim[b], Christian Meyer[a]

[a]*Department of Civil Engineering and Mechanical Engineering, Columbia University, SW 500 West 120th Street, New York, NY 10027, USA*
[b]*Department of Civil and Environmental Engineering, Hanyang University, 1271, Sa1-dong, Ansan 425-791, South Korea*

Abstract

Concrete bridge decks supported by main girders develop initial cracks in the longitudinal or transverse direction by applied loads. Therefore, it is important to consider the crack patterns and deflections if such decks are to be strengthened. This study investigated the effectiveness of strengthening using carbon fiber sheets. The experimental variables were the direction and the amount of strengthening material. To simulate the real behavior of the bridge deck, static structural tests were conducted on six specimens, with a built-in concrete girder on each side. The structural behavior was then observed through the crack pattern and the load–displacement relationship of each specimen. Also, the yield line theory that adopts the modified Johansen's yield criterion was applied to estimate the ultimate strength.
© 2003 Elsevier Science Ltd. All rights reserved.

Keywords: A. Carbon fiber sheet; B. Bridge deck; C. Yield line theory; D. Structural retrofit; D. Structural repair; D. Structural strengthening

1. Introduction

Bridge decks are structural members which support vehicle loads and transfer these to bridge girders. It is known that repeated application of vehicle loads can cause damage of both bridge deck and girders [1–3]. As the damage in the girder increases under repeated load application, so do the residual deformations, which in turn can cause damage in the deck, especially if there are large deformation differentials between adjacent girders. If such damage in the deck progresses sufficiently, it can eventually lead to failure [1–3]. For this reason it appears to be more critical to strengthen the deck rather than the girders of a deteriorated bridge [4,5]. Observations of actual bridges in service tend to support this assessment.

It is well known that a reinforced concrete deck, because of its deformational characteristics, carries concentrated wheel loads through two-way bending [6]. Therefore, if a strengthening material such as a carbon fiber sheet (CFS) is applied, which affects the slab bending strength and stiffness in one direction only, the amount of such strengthening as well as the orientation need to be considered very carefully [7–10].

The cracking patterns and failure modes caused by repeated load applications can be different from those due to monotonically applied loads [1–5]. Also the dynamic nature of the loads caused by moving vehicles can affect cracking and failure modes. It is the purpose of strengthening a bridge deck to assure that its load-carrying capacity, which may have deteriorated in time, be restored such that the deck can again safely resist the applied loads. Previous research conducted by Swamy et al. [11] determined that lapped plate, pre-cracking prior to strengthening and the presence of stress concentrations in the adhesive of strengthened concrete beams had no adverse effect on their structural behavior. Also, in a separate study by the authors [12], it was observed that it is possible to estimate the structural effectiveness of various strengthening materials applied to pre-damaged concrete deck panels [12]. In that test, some of the deck panels were loaded up to 60% of yielding loads of transverse rebars and then repaired by epoxy injection prior to strengthening. Other decks were loaded only up to initial cracking loads and not repaired at all. The test results showed that structural response to static loads was not influenced by the existence of pre-cracks.

---

* Corresponding author. Tel.: +212-854-6474; fax: +212-854-6267.
E-mail address: opera69@chollian.net (H. Oh).

This paper addresses the problem of strengthening bridge decks subjected to monotonically applied loads. A subsequent paper will deal with aspects of fatigue failure under repeated load applications [10]. Prototype deck panels were tested under static loads to evaluate different strengthening methods. Also the load-carrying capacity and failure patterns of strengthened decks are evaluated using yield line theory and are compared with test results.

2. Crack propagation in bridge deck

The crack propagation and failure behavior of bridge decks caused by moving vehicle loads is difficult to simulate numerically, especially if the various restraints and support conditions are taken into account. In general, the behavior of bridge decks supported by girders is dominated by one-way bending action. Therefore, the primary reinforcement is oriented perpendicular to the girders and direction of traffic. However, concentrated wheel loads by their very nature impose two-way bending, so that initial cracks in the bridge may form in either the transverse or the longitudinal direction, or both, Fig. 1 (steps 1 and 2). On the other hand, drying shrinkage and temperature gradients will generally cause cracks in the transverse direction.

If the load acting on a deck panel is increased monotonically, it will cause further crack propagation, generate new cracks, and eventually lead to either a flexural or a shear failure (Fig. 1). However, if a load is applied repeatedly, as in the case of a real bridge deck, the crack patterns and failure modes may be quite different, as flexure-shear and punching shear failure modes tend to dominate. This phenomenon will be explored elsewhere [10].

In the past, bridge decks have been strengthened in either the transverse or the longitudinal direction only, by applying CFS to the bottom surface along the entire length

of the bridge, because of the expected cracking of Step 1 in Fig. 1. However, the crack patterns of subsequent steps that have been observed in actual bridges in service are quite different. Therefore, such traditional strengthening techniques may be less than optimal. The experimental test program reported herein was planned to investigate in some detail failure modes of bridge decks that are strengthened in various different ways in order to improve the efficiency of such strengthening techniques.

3. Experimental study

The flexural strength of a singly reinforced concrete section is generally assumed to be

$$M_{n1} = A_s f_y \left(d - \frac{A_s f_y}{1.7 f_c' b} \right) \tag{1}$$

where A_s is the steel area, f_y is the yield strength, f_c' is the concrete strength, b is the unit slab width, and d is the distance from the tension steel to the compression face.

By applying a CFS to the tension face, additional moment capacity is being created, Fig. 2. The combined nominal flexural capacity is now

$$M_{n2} = A_s f_y \left(d - \frac{A_s f_y + A_{CFS} 0.8 f_{CFS}}{1.7 f_c' b} \right)$$
$$+ A_{CFS} 0.8 f_{CFS} \left(h - \frac{A_s f_y + A_{CFS} 0.8 f_{CFS}}{1.7 f_c' b} \right) \tag{2}$$

where A_{CFS} is the cross-sectional area of the CFS per unit width, and its average stress at failure assumed to be equal to 80% of its ultimate strength f_{CFS} [13], h is the total slab thickness.

Similar expressions can be derived for the deck strengthened in the longitudinal direction. According to
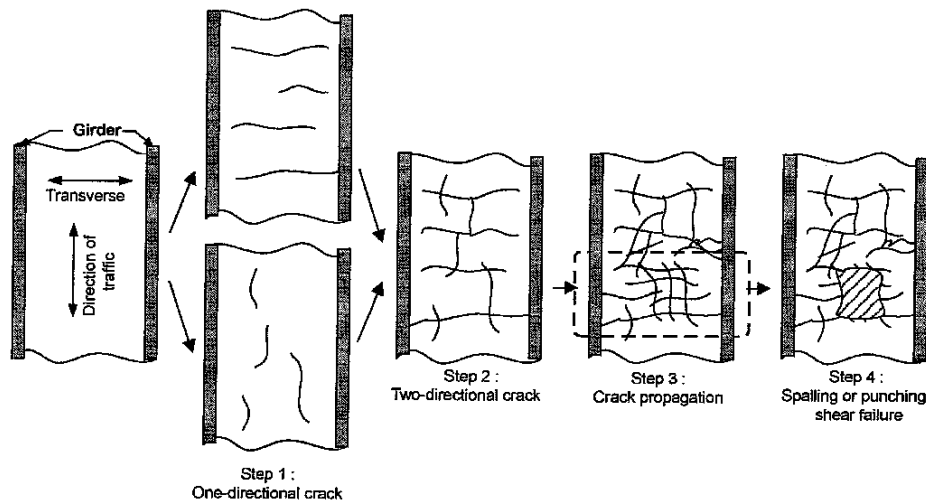

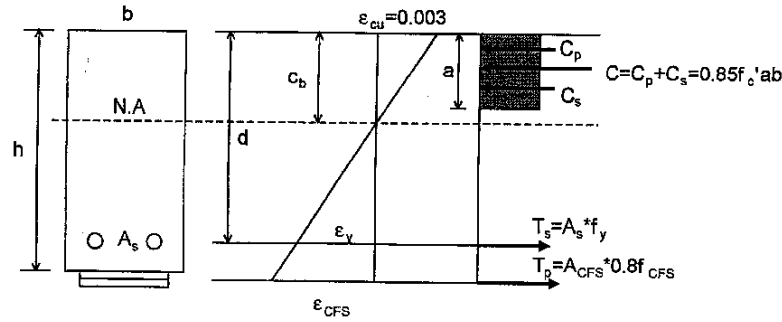Fig. 1. Typical failure steps of bridge deck.

Fig. 2. Strengthened RC section at failure.

the Korean Highway Design Specification [14], the transverse moment due to a concentrated wheel load P is given by

$$M = \frac{(L + 0.6)P(1 + \text{IM})}{9.6} \qquad (3)$$

where L is the clear span length between girders (in meters) and IM is the impact factor. Eq. (3) is based on the classical Westergaard theory [6]. When strengthening the section, it is useful to introduce a so-called strengthening ratio, defined as A_{CFS}/hb.

For the experimental test program, a prototype deck panel of dimensions $160 \times 240 \text{ cm}^2$ was selected to simulate a real bridge deck, supported by two girders, as shown in Fig. 3. The 28-day compressive strength of the concrete was 31 MPa. In the transverse direction, the deck reinforcing ratio was 0.551%. In the longitudinal direction, the reinforcement was about 67% of this amount, i.e. 0.367%. The material properties are listed in Table 1. Fig. 3 also shows the position of strain gages and LVDTs to measure strains and deflections.

The two strengthening variables considered in the experimental test program were the strengthening ratio and the direction of the CFS, i.e. transverse (T) or longitudinal (L). The specific strengthening patterns are shown in Fig. 4 (Table 2), i.e. the CFS are either applied over the entire soffit area or only in strips.
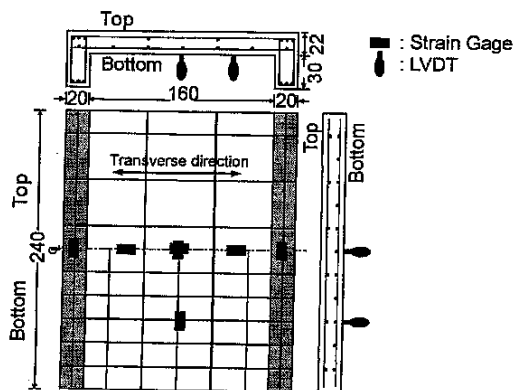

Fig. 3. Details of specimen (unit: cm).

The CFS were bonded to the prototype deck panel in an upside-down position as follows. To remove all laitance and smoothen the surface, the deck area was ground by hand and cleaned afterwards with air-pressure. A resin was applied as a primer by roller and cured for 24 h with a protective cover to keep it dry. After blending the epoxy adhesive in a suitable container, it was spread evenly over the bottom surface of the deck by roller. CFS were attached to the epoxy-coated surface, with the protective paper still in place, by pressing them into the epoxy with a rubber putter. After removing the protective paper, the sheets were further pressed into the epoxy coating with a screw type roller until they were completely immersed and no air voids between the concrete and the sheets remained. About 30 min to 3 h after the first epoxy application, another layer of epoxy was applied to assure that the CFS were completely immersed within the epoxy. The strengthened test panels were then cured for at least 10 days before testing. For panels with both longitudinal and transverse CFS strengthening, the CFS sheets in the longitudinal direction were attached first.

The static load was applied by a hydraulic jack of 2000 kN capacity to an area of $25 \times 50 \text{ cm}^2$ at the deck center to simulate the tire contact area of an actual vehicle, Fig. 5. During the test, displacements and strains in the strengthening material and reinforcing bars were measured by the gages shown in Fig. 3 and recorded automatically.

All six test panels were loaded up to 100 kN, unloaded, reloaded up to 200 kN, unloaded again, reloaded up to 300 kN, and unloaded again. Thereafter, panels CON and CS-L1 were loaded to failure, whereas the other four panels

Table 1
Material properties

	Yield strength	Ultimate strength (MPa)	Elastic modulus (MPa)	Ultimate strain
Concrete		31.0	25 900	0.003
Epoxy		88.3	7000	
Rebar	394	562	197 210	–
Carbon fiber	–	3500	231 722	0.015

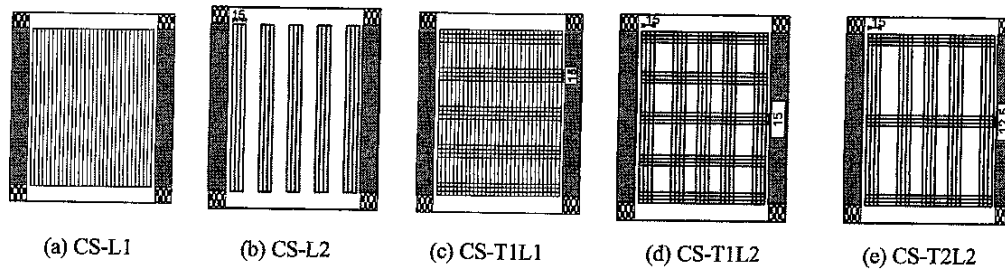(a) CS-L1　　　(b) CS-L2　　　(c) CS-T1L1　　　(d) CS-T1L2　　　(e) CS-T2L2

Fig. 4. Strengthening details in specimens.

were once more unloaded at 400 kN, before being loaded to failure.

4. Experimental test results

4.1. Crack patterns and failure modes

Fig. 6 shows the crack patterns of the six test panels at failure. The photo of Fig. 6(a) shows the cracks in the unstrengthened reference panel CON, whereas all the other images show the cracks in the CFS after panel failure. The crack patterns in the concrete were revealed after removal of the CFS but are not shown here.

In the unstrengthened test panel CON, failure was caused by biaxial bending. Initially, cracks developed in the longitudinal direction, and as the load increased further, also transverse cracks appeared, propagating from the initial longitudinal cracks, until failure. At failure, reinforcing bars yielded in both directions.

Failure of the CS-L1 specimen was initiated by diagonal cracking of the CFS near the panel quarter point. The carbon fibers experienced kinking across the crack without failure. In the case of the CS-L2 specimen, with only CFS strips in

the longitudinal direction, similar cracking occurred, but with smaller crack widths.

In panel CS-T1L1, the initial crack pattern was similar to the one in panel CS-L1, i.e. consisting of primarily longitudinal cracks. Unlike in the unstrengthened panel CON, the crack pattern remained essentially longitudinal, as the load increased. Prior to failure, the CFS ruptured, forming a dominant longitudinal crack, as is clearly shown in Fig. 6(d). Subsequently, the specimen failed in a punching-shear mode.

The cracking patterns of panels CS-T1L2 and CS-T2L2 were very similar. As in the reference panel CON, cracks propagated towards the deck edges, but crack widths were somewhat smaller than those of the other panels except for CON. Even after yielding of the steel reinforcement in both directions, no debonding of the CFS was observed. Both panels failed ultimately in biaxial bending.

4.2. Load–displacement relationships

Fig. 7(a) and (b) shows load–displacement relationships for all six test panels under the loading-unloading cycles described in Section 3. Panels CS-L1 and CS-L2

Table 2
Variables in experiment

Specimen	Strengthening ratio $((A_{CFS}/hb) \times 10^{-4})$		Strengthening direction
	Transverse (T)	Longitudinal (L)	
CON	–	–	
CS-L1	–	4.688	Longitudinal only, whole soffit area
CS-L2	–	2.344	Longitudinal only, strip type
CS-T1L1	1.875	4.688	Two-directional, whole soffit area and strip type
CS-T1L2	1.875	2.344	Two-directional strip type
CS-T2L2	0.9375	2.344	Two-directional strip type

Fig. 5. Test set-up.

(a) CON

(b) CS-L1

(c) CS-L2

(d) CS-T1L1

(e) CS-T2L2

(f) CS-T1L2
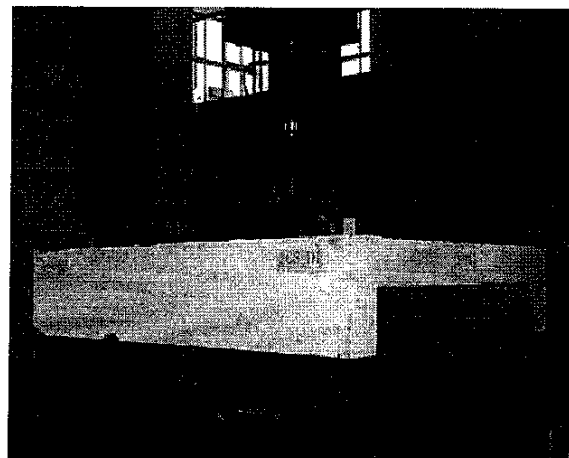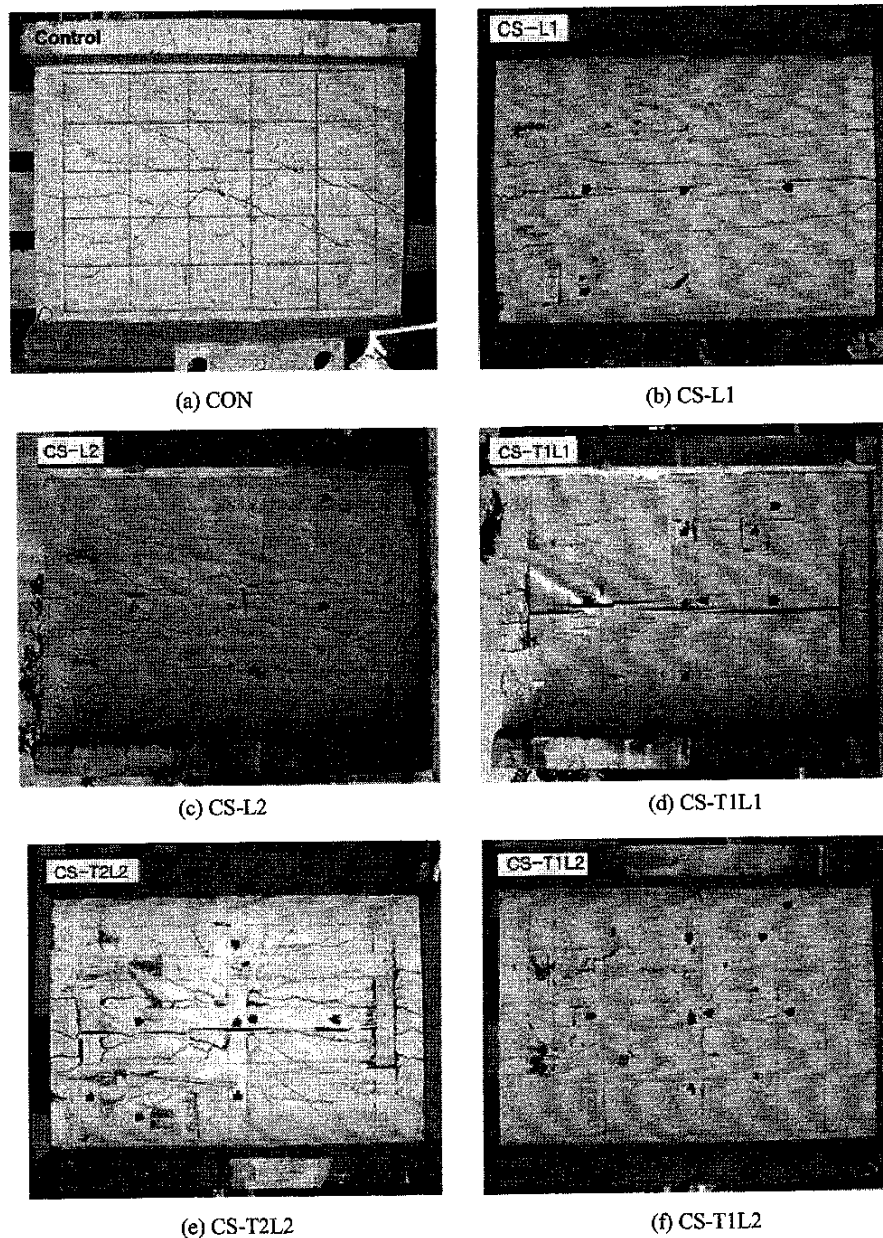
Fig. 6. Crack patterns of specimens.

exhibited very similar behavior as panel CON up to yielding of the transverse steel reinforcement (about 300 kN). The longitudinal rebars did not yield because the deck was strengthened by CFS in that direction. Compared with these three panels, the panels strengthened in both directions experienced increases in yield strength and stiffness. Also, with the exception of panel CS-T1L1, all biaxially strengthened panels displayed ductile failure modes and a large number of small cracks.

4.3. Load–strain relationships of rebars and CFS

The load–strain relationships for rebar and CFS are shown in Figs. 8 and 9. The unloading–reloading cycles are omitted for clarity. Some similarities and differences of results are compared in Table 3.

Transverse rebars in panel CS-L1 start yielding at a load of about 370 kN, which is slightly higher than the value experienced in panel CS-L2, Fig. 8(a) and Table 3a. Even though the amount of transverse reinforcement is the same
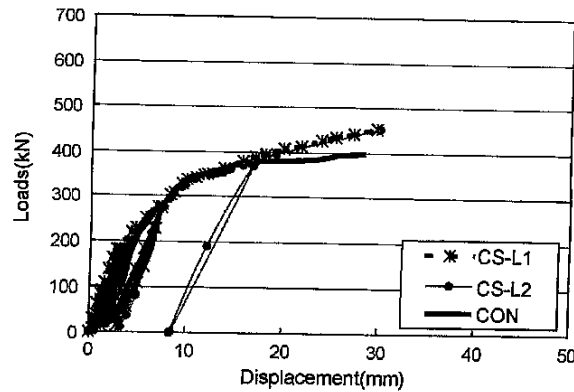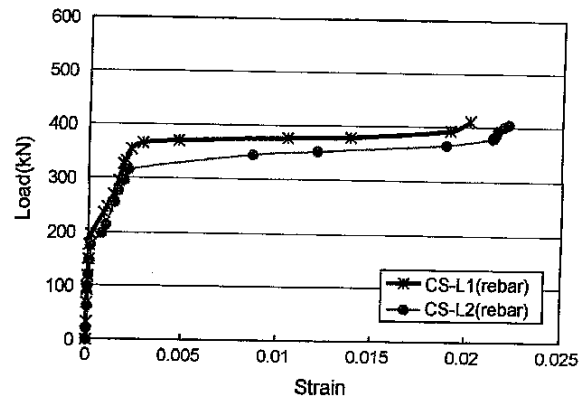
(a) One-directionally strengthened specimens
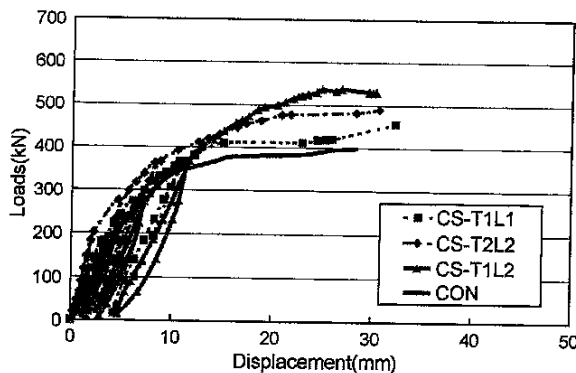
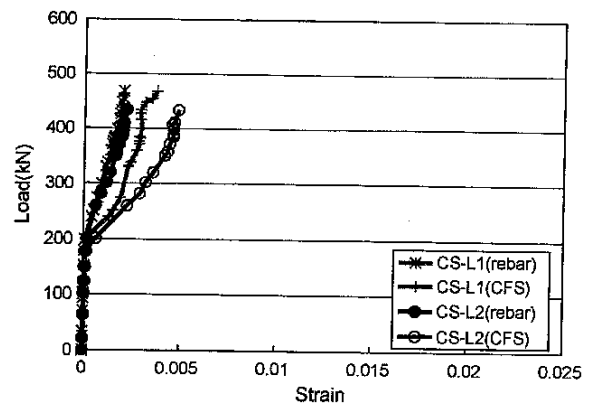(b) Two-directionally strengthened specimens

Fig. 7. Load–displacement relationships.

(a) the transverse direction

(b) the longitudinal direction

Fig. 8. Load–strain relationship of one-directionally strengthened specimens.

in both panels, the lower CFS strengthening in panel CS-L2 seems to affect the distribution between transverse and longitudinal moments. However, from Fig. 8(b) it is apparent that neither the longitudinal reinforcing bars nor the CFS experienced any significant strains and stresses for loading below 200 kN. Although the concrete developed initial cracks at about 150 kN, it took a considerable further load increase to force the load redistribution necessary to cause significant strains in the longitudinal steel and CFS. Since the CFS was further removed from the neutral plane, its strains were noticeably larger than those recorded for the reinforcing bars. Because panel CS-L2 was strengthened with much less CFS than panel CS-L1, the strains were correspondingly larger.

When comparing the curves for panel CS-L1 of Fig. 8 with those for panel CS-T1L1 of Fig. 9, which has been strengthened also in the transverse direction, one would expect a delay of yielding of the transverse reinforcement as a result. In fact, the transverse reinforcing bars of panel CS-L1 started to yield at a load of about 370 kN, while the corresponding load in panel CS-T1L1 was 350 kN. For inexplicable reasons the CFS in both the transverse and the longitudinal directions experienced the first large strain increase already at 150 kN, followed by a second change in slope at 300 kN. At about 430 kN, debonding occurred

between the concrete and the transverse CFS, whereupon the corresponding strain dropped to zero. The transverse CFS did not seem to affect the yielding of the transverse rebars, but have a restraining effect on the longitudinal CFS.

We can further gauge the effect of transverse strengthening by comparing the results for panel CS-L2 with those for CS-T1L2 and CS-T2L2 (Figs. 8 and 9, and Table 3b). Since panel CS-L2 was not strengthened in the transverse direction, the transverse rebar started to yield at a load of about 320 kN, whereas this occurred at 450 kN in panel CS-T1L2 with some transverse CFS strip and at 370 kN in panel CS-T2L2 with less transverse strengthening. Additional comparisons can be made in Table 3b concerning strains in the longitudinal rebars and CFS strips. Likewise, by comparing the results for the panel CS-T1L2 with those for CS-T1L1 and CS-T2L2, Table 3c, further insights can be gained into the effect of increasing longitudinal strengthening or reducing transverse strengthening. It might be pointed out that in panel CS-T1L2, the transverse CFS was directly bonded to the concrete surface and therefore more effective than those of panel CS-T1L1, in which the transverse CFS was bonded to the longitudinal CFS only.
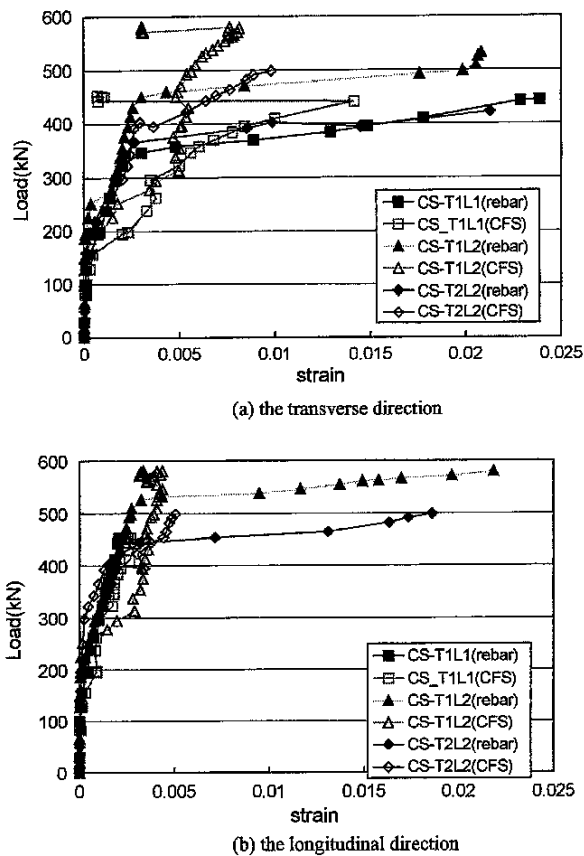
(a) the transverse direction

(b) the longitudinal direction

Fig. 9. Load and strain relationship of two-directionally strengthened specimens.

4.4. Strain distributions in CFS sheets

Figs. 10 and 11 display the strain distributions recorded in the CFS at various load levels. The initial behavior of

panel CS-L1 prior to crack propagation showed that the CFS was perfectly bonded to the concrete, but the macro crack propagation observed beyond a 300 kN load led to debonding and a redistribution between transverse and longitudinal directions.

In panel CS-T2L2 that was half as much strengthened in the transverse direction as panel CS-T1L2, a remarkable strain increment of almost 0.0085 in the transverse CFS occurred at 500 kN, whereas the corresponding strain in panel CS-T1L2 was only 0.0051. But the strains in the longitudinal directions were of almost equal magnitude. By comparing the strain increments between 300 kN (before yielding load of transverse rebar) and 500 kN (after or near the yield load), it becomes apparent that panel CS-T1L2 distributes stress very effectively.
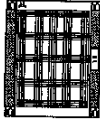
4.5. Load carrying capacity

In order to investigate the efficiency of the various strengthening techniques, 3-dimensional nonlinear finite element analyses were carried out before and after the physical experiments. The concrete slab was modeled with 8-node solid elements, reinforcing bars with beam elements, and the CFS was represented by membrane elements with stiffness properties only in the appropriate directions [15–19]. Both beam and membrane elements were assumed to be perfectly bonded to the concrete. The material properties were obtained experimentally. The rubber supports were simulated by spring elements with a hyperelastic material law.

The computed stress patterns of Fig. 12 are consistent with the crack patterns depicted in Fig. 6. It may be noticed that the stress contours for the unstrengthened specimen CON are very similar to those for specimen CS-T1L2 which was strengthened in two directions. This seems to indicate

Table 3a
Comparison with strain variation between CS-L1, CS-L2 and CS-T1L1

	Panel CS-L1	Panel CS-L2	Panel CS-T1L1
Transverse rebar			
Load at first slope change	200 kN	200 kN	150 kN
Strain at 350 kN	0.002	0.0023	0.002
Yield load (second slope change)	370 kN	320 kN	350 kN
Longitudinal rebar			
Load at first change slope	200 kN	200 kN	180 kN
Strain at 350 kN	0.0013	0.0015	0.002
Strain at 430 kN	0.0018	0.002	0.002
Longitudinal CFS			
Load at first slope change	200 kN	200 kN	150 kN
Strain at 350 kN	0.0025	0.004	0.002
Strain at 430 kN	0.0038	0.0045	0.0025

Table 3b

Comparison with strain variation between CS-L2, CS-T1L2 and CS-T2L2

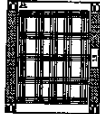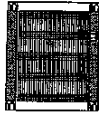|	Panel CS-L2	Panel CS-T1L2	Panel CS-T2L2
Transverse rebar			
Load at first slope change	200 kN	250 kN	200 kN
Strain at 350 kN	0.0023	0.002	0.0023
Yield load (second slope change)	320 kN	450 kN	370 kN
Longitudinal rebar			
Load at first slope change	200 kN	220 kN	220 kN
Strain at 350 kN	0.0015	0.0015	0.002
Strain at 450 kN	0.002	0.002	0.002
Longitudinal CFS			
Load at first slope change	200 kN	250 kN	300 kN
Strain at 350 kN	0.004	0.003	0.001
Strain at 450 kN	0.0045	0.0035	0.0025

that two-directional strengthening is more efficient than strengthening in only the transverse direction.

It is difficult to determine the load-carrying capacity of the strengthened deck, because this is a function of the type of loading, the type of strengthening, and the restraint conditions. Until now, only elastic beam theory or nonlinear finite element analyses have been employed in practice to estimate the capacity of strengthened bridge decks. Yet elastic beam theory is too simplistic to yield realistic results,

and nonlinear finite element analysis is too complex for practical design purposes.

For this reason it appears useful to provide a simple yet reasonably accurate analysis method as a third alternative. Yield Line Theory may be suitable for this task [20–22]. The different collapse mechanisms possible in strengthened bridge decks are shown in Fig. 13. The plastic moment capacity of a strengthened slab shall be designated as m_{uy} and m_{ux} along the longitudinal and transverse directions,

Table 3c

Comparison with strain variation between CS-T1L2, CS-T1L1 and CS-T2L2

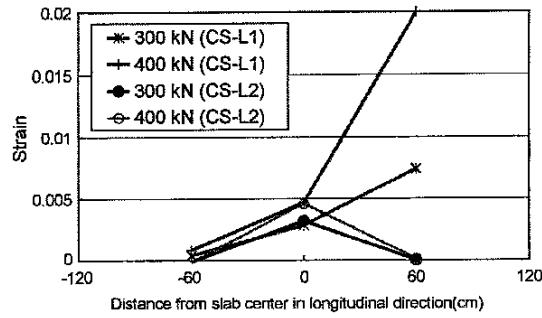|	Panel CS-T1L2	Panel CS-T1L1	Panel CS-T2L2
Transverse rebar			
Load at first slope change	250 kN	150 kN	200 kN
Strain at 350 kN	0.0023	0.003	0.0023
Yield load	450 kN	350 kN	370 kN
Longitudinal rebar			
Load at first slope change	220 kN	180 kN	220 kN
Strain at 350 kN	0.0015	0.0015	0.0015
Yield load (or peak load)	520 kN	430 kN (peak)	440 kN
Transverse CFS			
Load at first slope change	250 kN	150 kN	200 kN
Strain at 350 kN	0.005	0.005	0.003
Yield load (or peak load)	580 kN	430 kN (peak)	500 kN
Longitudinal CFS			
Load at first slope change	250 kN	150 kN	300 kN
Strain at 350 kN	0.003	0.002	0.001
Yield load (or peak load)	580 kN	450 kN	500 kN

Fig. 10. Load and strain distribution of CFS in the longitudinal direction on one-directionally strengthened specimens.

respectively. Note that this capacity is slightly less than the ultimate moment capacity of Eq. (2), because the reinforcing bars are assumed to have just reached the yield strain $\varepsilon_s = 0.002$, and neither the concrete nor the CFS have reached their failure strains yet.

The classical yield line solutions for slabs have been obtained for the case of isotropic reinforcement. Johansen has derived the so-called 'Affinity theorem', which enables solutions for orthotropic slabs to be obtained from those for isotropic slabs [20–22]. To determine the equivalent isotropic slab, the span lengths of the orthotropic slab and the loading are altered by a ratio that depends on the ratio of

Fig. 11. Loads and strain distribution of CFS on two-directionally strengthened specimens.

the ultimate moment capacities per unit width in the two directions: $\mu = m'_{uy}/m'_{ux} = m_{uy}/m_{ux}$, where the $'$-symbol denotes negative moment capacity. Then the orthotropic slab can be transformed to an equivalent isotropic slab known as the affine slab, using the affinity theorem: An orthotropic slab with negative and positive ultimate moment capacities of resistance per unit width in the x-direction (m'_{ux} and m_{ux}) and in the y-direction (m'_{uy} and m_{uy}), may be analyzed as an isotropic slab with negative and positive ultimate moments of resistance per unit width m'_{ux} and m_{ux}, in both directions, if the following transformations are carried out:

	Orthotropic	$\rightarrow$	Isotropic
Dimensions :	l_x	remains	l_x
	l_y	becomes	$\dfrac{l_y}{\sqrt{\mu}}$
Loading :	w_u	remains	w_u
	P_u	becomes	$\dfrac{P_u}{\sqrt{\mu}}$

where P_u is the ultimate concentrated load and w_u is the ultimate uniformly distributed load.

The ultimate load capacity depends on which type of yield line pattern of Fig. 13 is critical:

(a) Type 1:

$$P_u = 4(m_u + m'_u)\frac{b}{l} \tag{4}$$

(b) Type 2:

$$P_u = 8(m_u + m'_u)\frac{a}{l} + 2(m_u + m'_u)\frac{l}{a} \tag{5}$$

(c) Type 3:

$$P_u = 4(m_u + m'_u)\cot\frac{\phi_p}{2} + 2(m_u + m'_u)\phi_p \tag{6}$$

(d) Type 4:

$$P_u = 4(m_u + m'_u)\frac{b}{l}\cot\frac{\phi_p}{2} + 2m_u\phi_p \tag{7}$$

where b, l = dimensions of deck panel in longitudinal and transverse direction, respectively, $a = b/2$, ϕ_p = angle of the fan (in radian).

The solutions of Eqs. (4)–(7) may need to be modified if there exists an in-plane shear crack in the deck such as shown in Fig. 14 or a diagonal crack due to flexure. Any substantial relative motion of the two crack faces may introduce kinking of the CFS bands, Fig. 14, which reduces the contribution of the CFS sheet to the ultimate flexural strength of the section, because of the reorientation of the fibers. The reduction factor will be $\cos\alpha$, where α is
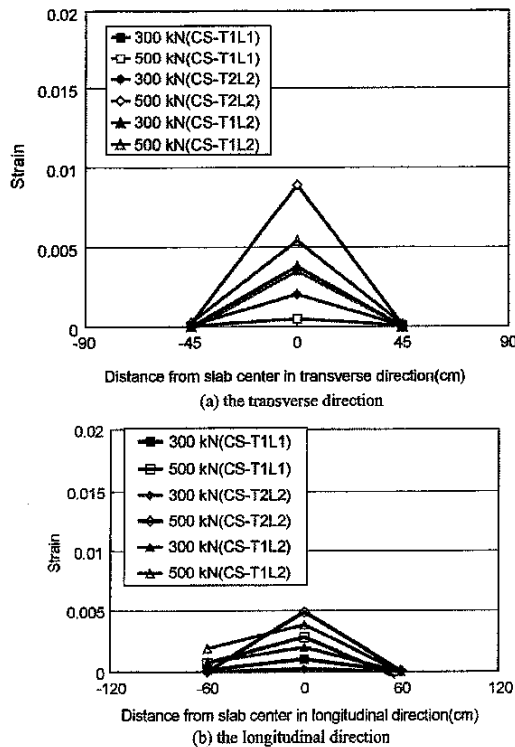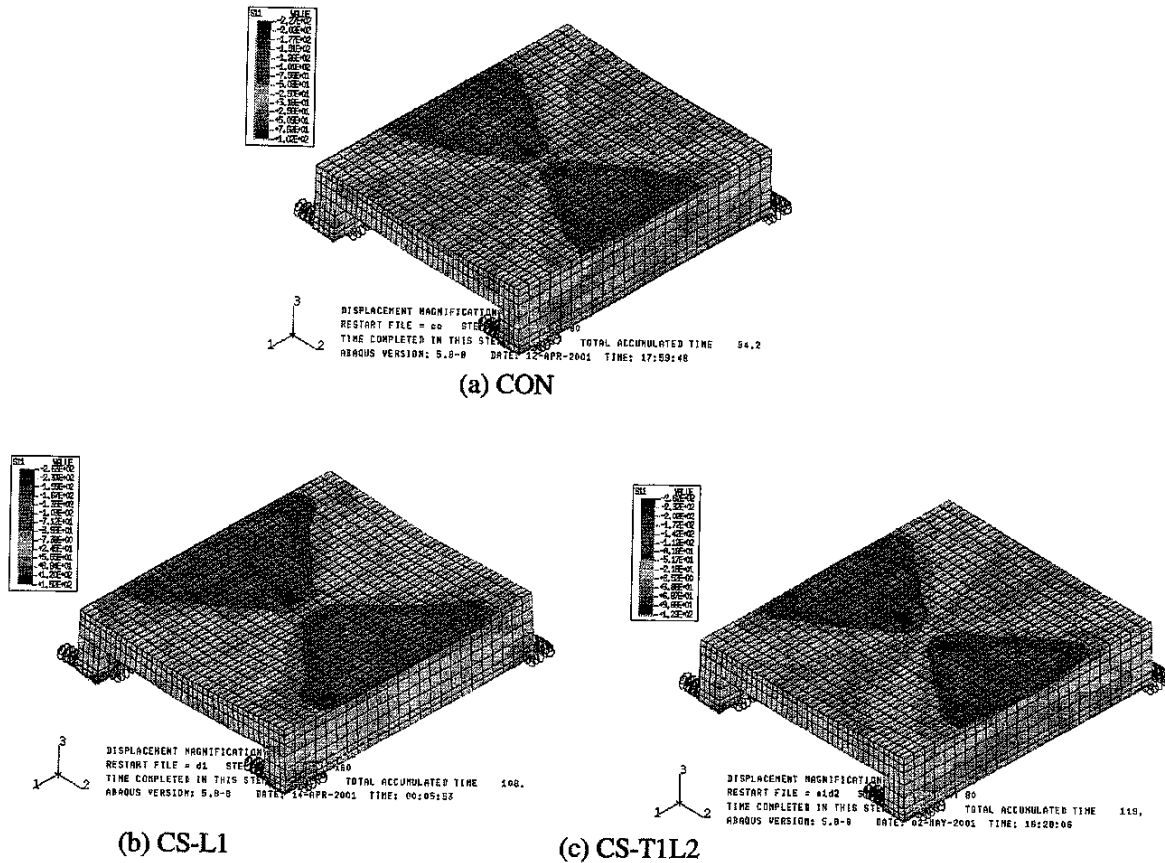
(a) CON

(b) CS-L1

(c) CS-T1L2

Fig. 12. Stress contours of deck specimens (FEA).

the angle between the normal to the crack and the fiber direction. Then, the yield moment and ultimate moment capacity per unit width can be computed as follows

$$M_{yx} = A_s f_y \left(d - \frac{A_s f_y + A_{CFS} f_{CFS}}{1.7 f'_c b} \right)$$
$$+ A_{CFS} f_{CFS} \left(h - \frac{A_s f_y + A_{CFS} f_{CFS}}{1.7 f'_c b} \right) \tag{8}$$

$$M_{ux} = A_s f_y \left(d - \frac{A_s f_y + A_{CFS} 0.8 f_{CFS} \cos \alpha}{1.7 f'_c b} \right)$$
$$+ A_{CFS} 0.8 f_{CFS} \cos$$
$$\times \alpha \left(h - \frac{A_s f_y + A_{CFS} 0.8 f_{CFS} \cos \alpha}{1.7 f'_c b} \right) \tag{9}$$

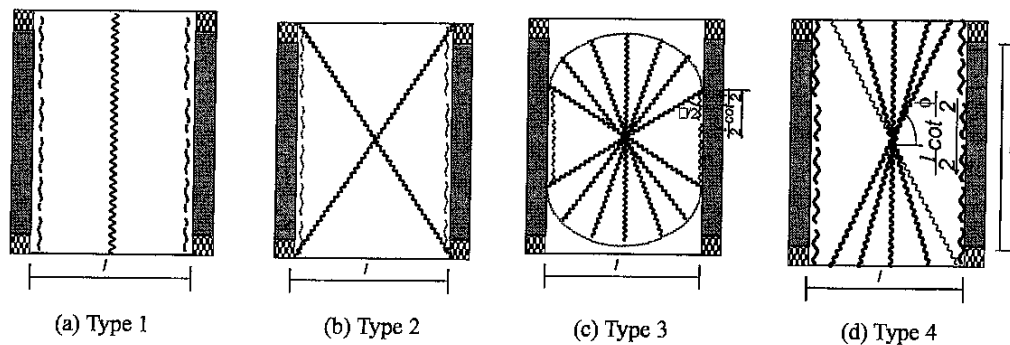where f_{CFS} = stress of CFS when rebar starts yielding.

(a) Type 1

(b) Type 2

(c) Type 3

(d) Type 4

Fig. 13. Supposed yield lines of deck.
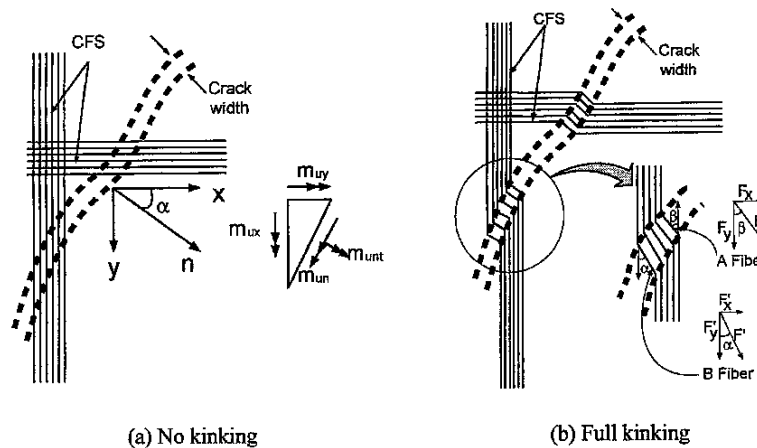
(a) No kinking   (b) Full kinking

Fig. 14. Kinking of CFS at crack face.

Table 4
Comparison between experimental and theoretical results

Specimen	Failure mode	Yield load (kN) (rebar's yield point)		$\dfrac{\text{Theory}}{\text{Test}}$	Failure load (kN) (CFSs rupture or kinking)		$\dfrac{\text{Theory}}{\text{Test}}$
		Test	Theory		Test	Theory	
CON	Flexural-shear	405 (Type 4)	378 (Type 4)	0.93	–	–	
CS-L1	Compressive	470 (Type 1)	468 (Type 1)	1.00	583 (Type 1)	605 (Type 1)	1.04
CS-L2	Flexural-shear	442 (Type 3)	459 (Type 3)	1.04	583 (Types 1, 3)	583 (Type 3)	1.00
CS-T1L1	Punching-shear	481 (Type 1)	547 (Type 2)	1.14	573 (Punching shear)	740 (Type 2)	1.29
CS-T2L2	Flexural-shear	450 (Type 4)	458 (Type 4)	1.02	605 (Type 4)	573 (Type 4)	0.95
CS-T1L2	Flexural-shear	520 (Type 4)	454 (Type 2)	0.87	638 (Type 2)	626 (Type 2)	0.98

Experimental and theoretical results are shown in Table 4. As can be seen, discrepancies between theory and experiment do not exceed 14%, except for panel CS-T1L1, which failed in punching shear, so that yield line theory was not applicable. Compared with the reference panel CON, strengthening increased the yield strength from 9% (panel CS-L2) to 28% (CS-T1L2). If we define as failure the steel yielding in the unstrengthened reference panel CON and rupture or kinking of the CFS sheets in the case strengthened panels, then the strength increases due to the CFS sheets ranged from 41% (panel CS-T1L1) to 58% (panel CS-T1L2). According to the results panels CS-T2L2 and CS-T1L2 appear to exhibit the best strengthening solutions. Although panel CS-T1L2 utilizes less CFS material than CS-T1L1, both yield and ultimate strengths are higher, because the strengthening pattern of panel CS-T1L1 leads to a punching shear failure.

patterns of the strengthened panels depend on the strengthening pattern.

Yield line theory can be used to predict with reasonable accuracy the load-carrying capacity of bridge decks, even if these are strengthened with CFS sheets. For the determination of the amount of strengthening needed to improve the load-carrying capacity of deteriorated deck panels, this theory is more effective than either traditional beam theory or FE analysis.

The load carrying capacity of panel CS-T1L2, which was strengthened in two directions, was 56% higher than that of the unstrengthened reference panel CON. This seems to indicate that two-directional strengthening with CFS strips is more effective than any other strengthening scheme, including the scheme of panel CS-T1L1, in which twice as much CFS material was applied in the longitudinal direction.

5. Conclusions

The results presented here lead to the following conclusions. Strengthening concrete bridge deck panels with CFS can substantially increase their load-carrying capacity, flexural stiffness and reduce cracking. The cracking

References

[1] Sonoda K, Horikawa T. Fatigue strength of reinforced concrete slab under moving loads. IABSE Rep 1982;37:455–62.
[2] Schläfli M, Brühwiler E. Fatigue of existing reinforced concrete bridge deck slabs. Engng Struct 1998;20(11):991–8.

[3] Mufti AA, Jaeger LG, Bakht B, Wegner LD. Experimental investigation of fibre-reinforced concrete deck without internal steel reinforcement. Can J Civil Engng 1993;20(3):398–406.

[4] Takeshi H. An outline of repairing and strengthening of RC deck slabs. Bridge Found Engng 1994;26(8):105–8.

[5] Fang IK, Worley JA, Burns NH, Klinger RE. Behavior of isotropic R/C bridge decks on steel girders. J Struct Engng 1990;116(3):659–78.

[6] Westergaard HM. Computation of stresses in bridge deck slab due to wheel loads. Public Roads 1930;11(1):1–23.

[7] Quantrill RJ, Hollaway LC, Throne AM. Experimental and analytical investigation of FRP strengthened beam response. Mag Concrete Res 1996;48:331–42.

[8] Saadatmanesh H, Wei A, Ebsnni MR. RC beams strengthened with GFRP plate I: experimental study. J Struct Engng 1991;117(11):3417–33.

[9] Swamy RRN, Jones R, Charif A. The effect of external plate reinforcement on the strengthening of structurally damaged RC beams. Struct Engnr 1989;67(3):45–56.

[10] Sim J, Sim JW, Oh HS, Lee KM. Fatigue loading effect on the strengthening concrete bridge deck specimen with carbon fiber sheet. Proceeding of EASEC-8 2001; Paper No.1529.

[11] Swamy RRN, Jones R, Bloxham JW. Structural behavior of reinforced concrete beams strengthened by epoxy-bonded steel plate. Struct Engnr 1987;56A(2):59–68.

[12] Sim J. Strengthening effect of reinforced concrete bridge deck. Research report. Korea Highway Corporation, Korea 2000 (in Korean).

[13] Bae IH. Flexural analysis and design of R/C beams strengthened with steel plate or carbon fiber composites. PhD Dissertation. Hanyang University; 1998 (in Korean).

[14] Korea's Ministry of Construction and Transportation. Korean Highway Design Specification; 1996.

[15] Hsu TTC. Unified theory of reinforced concrete. Boca Raton, FL: CRC Press; 1993. p. 205–18.

[16] Hu MT, Schmobrich WC. Nonlinear finite element analysis of reinforced concrete plate and shells under monotonic loading. Comput Struct 1991;38(16):637–51.

[17] Willam KJ, Mentrey Ph. Triaxial failure criterion for concrete and its generalization. ACI Struct J 1995;92(3):311–8.

[18] Comite Euro-International Du Beton. CEB-FIP model code. Thomas Telford; 1993.

[19] Shahrooz BM, Ho AE, Aktan AE. Nonlinear finite analysis of deteriorated RC slab bridge. ASCE J Struct Engng 1992;120(2):422–40.

[20] Park R, Gamble WL. Reinforced concrete slab, 2nd ed. New York: Wiley; 2000.

[21] Johansen KW. Yield line theory. London: Cement and Concrete Association; 2000.

[22] Nielsen MP. Limit analysis and concrete plasticity, 2nd ed. Boca Raton, FL: CRC Press; 1999.